






 Cite this: *RSC Adv.*, 2020, **10**, 37800

Effect of van der Waals interactions on the adhesion strength at the interface of the hydroxyapatite–titanium biocomposite: a first-principles study†

 Irina Yu. Grubova, ^{*a} Maria A. Surmeneva, ^a Roman A. Surmenev ^{*a} and Erik C. Neyts ^b

Hydroxyapatite (HAP) is frequently used as biocompatible coating on Ti-based implants. In this context, the HAP-Ti adhesion is of crucial importance. Here, we report *ab initio* calculations to investigate the influence of Si incorporation into the amorphous calcium-phosphate (a-HAP) structure on the interfacial bonding mechanism between the a-HAP coating and an amorphous titanium dioxide (a-TiO₂) substrate, contrasting two different density functionals: PBE-GGA, and DFT-D3, which are capable of describing the influence of the van der Waals (vdW) interactions. In particular, we discuss the effect of dispersion on the work of adhesion (W_{ad}), equilibrium geometries, and charge density difference (CDD). We find that replacement of P by Si in a-HAP (a-Si-HAP) with the creation of OH vacancies as charge compensation results in a significant increase in the bond strength between the coating and substrate in the case of using the PBE-GGA functional. However, including the vdW interactions shows that these forces considerably contribute to the W_{ad} . We show that the difference ($W_{ad} - W_{ad}(vdW)$) is on average more than 1.1 J m⁻² and 0.5 J m⁻² for a-HAP/a-TiO₂ and a-Si-HAP/a-TiO₂, respectively. These results reveal that including vdW interactions is essential for accurately describing the chemical bonding at the a-HAP/a-TiO₂ interface.

Received 9th July 2020

Accepted 28th September 2020

DOI: 10.1039/d0ra06006b

rsc.li/rsc-advances

Introduction

In recent years, ceramics based on hydroxyapatite (HAP, Ca₁₀(PO₄)₆(OH)₂) are commonly considered as coating materials on metallic implants and scaffolds for tissue engineering because of their biocompatible and osteoconductive properties.^{1,2} The most commonly used substrates for HAP coating deposition are titanium (Ti) and its alloys, which are clinically used as metal implants due to their good bulk properties, such as relatively low modulus, good fatigue strength, and high corrosion resistance.^{3–5} By properly selecting the processing parameters of coating formation, a strong bonding of the ceramic coating to the substrate can be achieved. Nevertheless, during the surgical

implantation and clinical use of a high-loaded bone implant, the ceramic coating can chip or delaminate from the metal surface for a number of reasons, which might cause the implant rejection. From a clinical perspective, this is to be avoided at all cost. As a result, improving the adhesion of such kind of metal-ceramic interfaces remains an important problem. There are some commonly accepted guidelines regarding how to enhance the adhesion at the HAP/Ti interface,⁵ including a denser microstructure and thinner HAP coatings resulting in high bonding strength,^{6,7} reducing the residual stress,⁸ doping HAP with other elements such as Si, Sr, and Ag,^{6,9} controlling the Ti substrate surface texture and compositions,^{10,11} and controlling the choice of deposition method and its operating conditions.^{12,13}

Although the large number of research groups actively work in the field of studying and applying thin biocompatible ceramic coatings, it is nevertheless still difficult to quantitatively comprehend the detailed interatomic interaction mechanism at the Ti-ceramic coating interface by conventional experimental methodologies.

Nevertheless, various theoretical approaches, such as density functional theory (DFT) can provide complementary understanding of the interfacial structure and the electronic properties of the interface, which no experimental technique can directly reach.

^aResearch Center for Physical Materials Science and Composite Materials, Research School of Chemistry & Applied Biomedical Sciences, National Research Tomsk Polytechnic University, Lenin Avenue, 30, 634050 Tomsk, Russia. E-mail: rodeo_88@mail.ru; rsurmenev@gmail.com

^bDepartment of Chemistry, PLASMANT Research Group, NANOLab Center of Excellence, University of Antwerp, Universiteitsplein 1, B-2610 Wilrijk, Antwerp, Belgium

† Electronic supplementary information (ESI) available: Two views of the phase-pure HA unit cell with the labelled phosphate and hydroxyl groups, Fig. S1. The calculated W_{ad} for 24 constructed interfaces between aSiHA and aTiO₂, Table S1. See DOI: 10.1039/d0ra06006b



In standard DFT approaches, such as local-density approximation (LDA) and the generalized gradient approximation (GGA), the functionals provide an accurate description of physical properties of many atoms, molecules, and solids. However, these approximations fail to reproduce non-local dispersive forces, generally denoted as van der Waals (vdW) interactions, whose role is obviously important for the study of the interactions at the interfaces.

In recent years, several functionals were developed to consider vdW forces for the description of the adhesion mechanism correctly. The most successful and commonly used approaches are the dispersion-corrected DFT (DFT-D)^{14–24} and the vdW density functional (vdW-DF).²⁵ Among them, the so-called DFT-D3 method was successfully used in both molecular and solid-state applications.²⁶ The main advantage of DFT-D3 is that it is obtained at negligible computational cost, which makes it particularly attractive in applications to large systems.²⁷ The DFT-D3 method,²⁶ proposed by Grimme *et al.* in 2010, suggests to define the dispersion correction energy between two atoms *i* and *j* as:

$$E_{ij}^{\text{vdW}} = s_6 f_6(r_{ij}) \frac{C_6^{ij}}{r_{ij}^6} + s_8 f_8(r_{ij}) \frac{C_8^{ij}}{r_{ij}^8}. \quad (1)$$

In this formalism, damping of the following form is used:

$$f_n(r_{ij}) = \frac{s_n}{1 + 6[r_{ij}/(s_{r,n} R_{ij})]^{-\alpha_n}}, \quad (2)$$

here, s_n , $s_{r,n}$, and α_n are empirical parameters; $R_{ij} = \sqrt{\frac{C_8^{ij}}{C_6^{ij}}}$ is the cutoff radius associating with the pair of atoms *i* and *j*.

This paper is a continuation of our previous *ab initio* study²⁸ of interface interactions in HAP/Ti composites that was concentrated foremost on the effect of substitutional Si doping in the amorphous calcium-phosphate (a-HAP) structure on the work of adhesion (W_{ad}), integral charge transfer, charge density difference (CDD) and theoretical tensile strengths between an a-HAP coating and amorphous titanium dioxide (a-TiO₂) substrate.

The results revealed that the presence of Si dopants in the a-HAP (a-Si-HAP) structure strongly alters not only the bioactivity and resorption rates, but also the mechanical properties of the studied interface.

However, despite the obtained insight gained into the nature of the adhesion mechanism between a-HAP and a-TiO₂, the effect of the vdW forces on the adhesion mechanism is still unclear, because of the GGA functional limitations, and further study of the description of vdW interaction within the DFT approach is needed.

Although numerous studies have been devoted to the atomistic simulation of HAP properties, only a few theoretical studies have analyzed the mechanism of the HAP interaction with Ti at the coating/substrate interface. Moreover, no studies to date have examined how the incorporation of Si affects such nanoscale properties as vdW interactions, which can be critical to the determination of the interfacial adhesion mechanism of

the HAP/Ti composites and cannot be reached by experimental approach.

Therefore, here we focus on the a-HAP/a-TiO₂ and a-Si-HAP/a-TiO₂ interface interactions with the aim of comparing results obtained with a reliable vdW functional to the results obtained with the PBE-GGA functional, which are conventionally used to describe only chemical bonding.

Thus, this paper aims to describe the adhesion mechanism with a rigorous treatment of non-local interactions as well as the effect of dispersion forces on the equilibrium geometries of studied interfaces and the role of these forces in the binding mechanism.

Calculation method

Our calculations are based on DFT as implemented in VASP (Vienna *Ab initio* Simulation Package).^{29–36} VASP is a complex package for simulation of many-electron systems at an atomic scale, which is widely applied for the numerical solution of the challenges of quantum mechanical molecular dynamics and calculations related to the electronic structure. The exchange-correlation interactions are treated at the GGA level, employing the Perdew–Burke–Ernzerhof (PBE) functional^{34,35} using plane-wave basis sets and the projector-augmented wave method as implemented in VASP.^{33,36} The plane-wave cutoff is set to 550 eV, valence electrons are 1s¹ for hydrogen, 3s²3p³ for phosphorus, 3s²3p⁶4s² for calcium, 2s²2p⁴ for oxygen, 3s²3p² for silicon, and 3d³4s¹ for Ti. The total energy in the calculations is converged to within 0.01 eV, and a 6 × 6 × 1 *I*-centered *k*-point grid is used for *k*-point sampling. The DFT-D3 method is used to account for dispersion corrections. A detailed description of the construction of the considered interfaces and the amorphization procedure can be found in our previous works^{28,37} and ESI.† The atomic structures are visualized by the VESTA 3 program.³⁸

Results and discussion

In our previous work,²⁸ we studied the effects of Si-doping on the adhesion mechanism and ideal tensile strength of fully relaxed a-HAP/a-TiO₂ interface structures using a GGA functional. For creating the Si substituted interfaces we used the a-HAP/a-TiO₂ model with two possible stacking positions, which resulted in the best interatomic interaction.³⁷

In this study, the aim is to improve our understanding of the interaction between the a-HAP coating and the a-TiO₂ substrate. For this purpose, we focus on the comparison of the results obtained for two best stacking positions of each considered interfaces, and calculated with normal GGA and dispersion-corrected DFT-D3 functionals. The initial geometry of the studied interfaces are presented in Fig. 1.

Initially, the preferred configuration of the interfaces was determined by quantifying the adhesion interaction, which is characterized by the W_{ad} , within the GGA approximation. By neglecting diffusion and plastic deformation, W_{ad} of an interface can be defined by eqn (3):³⁹

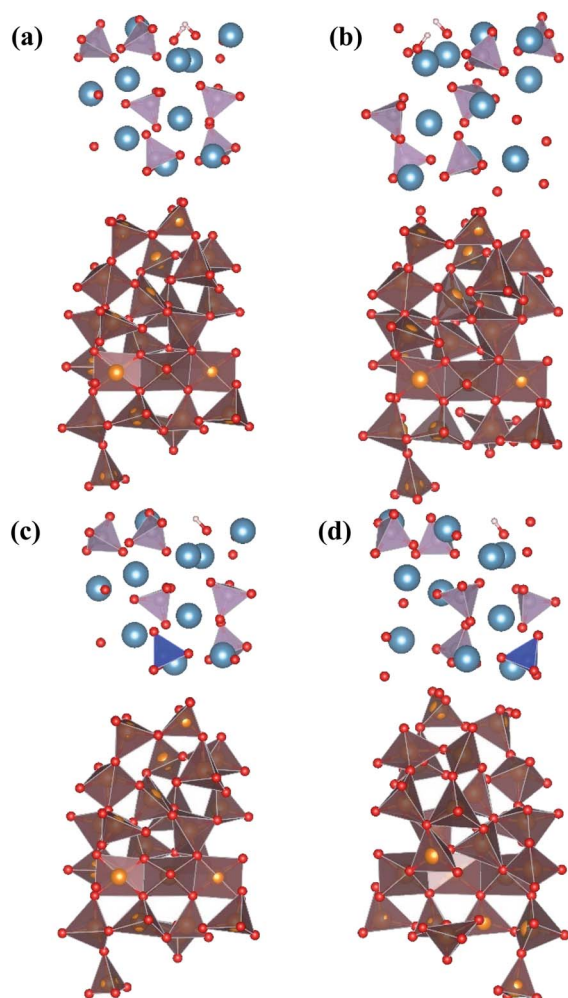


Fig. 1 Side view of the structural models of a-HAP/a-TiO₂ (a and b) and a-Si-HAP/a-TiO₂ (c and d) interfaces before relaxation for stacking I (a and c) and II (b and d). Red spheres, O; blue, Ca; white, H; violet, P; dark blue, Si; orange, Ti.

$$W_{\text{ad}} = \frac{1}{NA} [E_{\text{tot}(\text{int})} - E_{\text{tot}(\text{a-HAP})} - E_{\text{tot}(\text{a-TiO}_2)}], \quad (3)$$

where $E_{\text{tot}(\text{int})}$ is the total energy of the interface system in its optimized geometry, $E_{\text{tot}(\text{a-HAP})}$ and $E_{\text{tot}(\text{a-TiO}_2)}$ are the total energies of the isolated component slabs (substrate and coating) with the same geometry as that of the optimized interface system, and A ($A = 58.5471 \text{ \AA}^2$) is the interface surface area. The factor N in eqn (3) accounts for the presence of one interface (in our case the $N = 1$, and hence the a-HAP/a-TiO₂ interface model contains a single interface).

The results are shown in Table 1. As can be seen in the table, including dispersion interactions in our calculations *via* the DFT-D3 functional significantly changes the obtained values of W_{ad} . The higher the absolute value of the obtained W_{ad} is, the more stable the interfacial bonds.

The first feature to highlight is that for the PBE functional we can observe that the Si substitution strongly increases the interaction at the interface for both stacking positions, indicating that the Si-doped a-HAP surface is more reactive. The

Table 1 Work of adhesion calculated with various exchange-correlation functional

Functional	$W_{\text{ad}} (\text{J m}^{-2})$			
System	a-HAP/a-TiO ₂		a-Si-HAP/a-TiO ₂	
	I	II	I	II
Functional				
PBE	−0.690	−2.030	−1.370	−2.855
DFT-D3	−1.740	−0.930	−0.870	−2.315

increase of W_{ad} is about 50% and 30% for stacking I and II, respectively. The obtained data are in good agreement with experimental results,⁴⁰ where doping the HAP structure by Si was shown to lead to a decrease in crystal size and an increase in their specific surface, which in turn determined the improvement in the sorption properties of HAP. Also to note is the discrepancy between the results obtained with the different DFT functionals considered in this work. The less negative W_{ad} were computed with the DFT-D3 approach for the a-Si-HAP/a-TiO₂. However, in the case of a-HAP/a-TiO₂, DFT-D3 correction lead to the W_{ad} larger than those obtained from the PBE-GGA scheme for the stacking I and lower for the stacking II.

Thus, the semi-empirical method proposed by Grimme describes the effect of dispersion forces on the interatomic interaction at the considered interfaces. Analysis of the calculated data shows that the contribution of the vdW interactions is rather high, since the value of $(W_{\text{ad}} - W_{\text{ad}}(\text{vdW}))$ is on average more than 1.1 J m^{-2} and 0.5 J m^{-2} for a-HAP/a-TiO₂ and a-Si-HAP/a-TiO₂, respectively.

Interactions at the interface lead to charge redistribution due to electronic hybridization between the orbitals of the coating and the substrate. Therefore, for gaining a better insight in the influence of Si doping in the a-HAP structure with and without dispersion DFT on the electronic interactions at the studied interfaces, the CDD was evaluated as follows:⁴¹

$$\Delta\rho(r) = \rho_{\text{a-HAP/a-TiO}_2}(r) - \rho_{\text{a-HAP}}(r) - \rho_{\text{a-TiO}_2}(r), \quad (4)$$

where $\rho_{\text{a-HAP/a-TiO}_2}(r)$ is the charge density of the total a-HAP/a-TiO₂ interface system, and $\rho_{\text{a-HAP}}(r)$ and $\rho_{\text{a-TiO}_2}(r)$ are the charge densities for the isolated a-HAP and a-TiO₂ slabs, respectively.

CDD with isosurface values of $\pm 0.002 \text{ eV \AA}^{-3}$ for a-HAP/a-TiO₂ and a-Si-HAP/a-TiO₂ systems plotted for both functionals (PBE, DFT-D3) are shown in Table 2. The isosurfaces of charge redistribution at the interface indicate that the electron charge was mainly localized in two near-boundary layers. The plotted CDD helps to understand the chemical bonding mechanism at the constructed interfaces. The yellow and the blue areas represent the depletion and accumulation of electrons, respectively. For all interfaces, we observe a charge depletion near the O atoms from the a-TiO₂ slabs and a charge accumulation near the Ca atoms, which means that covalent Ca–O bonds are formed. The same character of the charge transfer is observed between O atoms from the PO₄ groups and Ti atoms along the Ti–O direction at the interface.

Table 2 Charge density difference (CDD) for the a-HAP/a-TiO₂ interface and the a-Si-HAP/a-TiO₂ interface. The isosurface value is set to $\pm 0.002 \text{ e \AA}^{-3}$. Yellow regions show electron depletion, and cyan regions represent electron accumulation. Interfacial bonding is shown as black dashed ovals

		a-HAP/a-TiO ₂	a-Si-HAP/a-TiO ₂
Stacking position I	PBE		
	DFT-D3		
Stacking position II	PBE		
	DFT-D3		

Further, it can be seen that Ti and Ca atoms act as electrons acceptors (Lewis acid), whereas O atoms from the coating and the a-TiO₂ slab act as electrons donors (Lewis base). The obtained results are consistent with those reported in our previous DFT studies.

The calculations show that the character of interactions at the a-HAP/a-TiO₂ strongly depends on Si dopants and the used DFT functionals. Based on the visualization of CDD, for a-HAP/a-TiO₂ there is one Ti–O bonds for both stacking positions in the range of 1.83–2.03 Å. Moreover, three covalent Ca–O bonds in the range of 2.36–2.61 Å were detected in the case of using the DTF-D3 approach (for both stacking positions) and PBE functional (for stacking position II) for a-HAP/a-TiO₂. Nevertheless, a-HAP/a-TiO₂ with the stacking position I calculated with the PBE method shows only one covalent Ca–O bond (2.29 Å) (Table 2).

As for the a-Si-HAP/a-TiO₂ case for both stacking positions, the use of the DFT-D3 functional leads to the reduction of the amount of bonds, which in turn decreases the adhesion strength at the interface. The a-Si-HAP/a-TiO₂ interface (stacking I, PBE) shows one Ti–O bond and two Ca–O bonds with lengths less than 2.58 Å. One Ti–O bond (1.99 Å) and three Ca–O bonds in the range of 2.19–2.49 Å were generated across the a-Si-HAP/a-TiO₂ (stacking II, PBE) interface, showing the quite strong chemical bonding at the interface (Table 2).

The structural picture of the interaction at the a-Si-HAP/a-TiO₂ (stacking I, DFT-D3) shows two Ca–O bonds of about 2.40 ± 0.03 Å. One Ti–O bond (2.76 Å) and two Ca–O bonds (2.29 and 2.25 Å) formed at the a-Si-HAP/a-TiO₂ (stacking II, DFT-D3) interface. Thus, this structural analysis reveals that the dispersion forces induce the observed change in the W_{ad} values. The change in adhesion at the interface depends not only on the composition, but also on the stacking positions. The bond

lengths are mainly determined by a balance between the long-range attractive vdW forces and the short-range Pauli repulsion.

Conclusion

In this study, first-principles calculations are performed to investigate the influence of Si dopants on the interfacial adhesion of the a-HAP/a-TiO₂ interface, contrasting two different density functionals: PBE-GGA, and DFT-D3, which is capable of describing the influence of the dispersion forces on the interfacial bonding mechanism. The W_{ad} value of various interface models with different stacking configurations and compositions are evaluated. Our calculations indicate that the Si-doping in the HAP crystal has a large impact on the adhesion properties of the a-HAP/a-TiO₂ interface. In the case of a-Si-HAP/a-TiO₂ the use of the DFT-D3 functional yields less negative values for W_{ad} than the PBE-GGA functional. However, in the case of a-HAP/a-TiO₂ interface, the final adhesion at the interface depends also on the stacking position. Moreover, the adhesion mechanism is mainly supported by the formation of covalent (polar) Ca–O and Ti–O bonds across the interface.

Thus, we can conclude that dispersion interactions play a significant role in altering the adhesion mechanism and charge distribution, and accounting for such interactions is critical in molecular simulations.

Conflicts of interest

There are no conflicts to declare.

Acknowledgements

The authors gratefully acknowledge financial support from the Russian president's grant MK-330.2020.8 and BOF Fellowships for International Joint PhD students funded by University of Antwerp (UAntwerp, project number 32545). The work was carried out at Tomsk Polytechnic University within the framework of Tomsk Polytechnic University Competitiveness Enhancement Program grant and in part using the Turing HPC infrastructure of the CalcUA core facility of the UAntwerp, a division of the Flemish Supercomputer Centre (VSC), funded by the Hercules Foundation, the Flemish Government (department EWI) and the UAntwerp, Belgium.

References

- 1 A. Vladescu, M. A. Surmeneva, C. M. Cotrut, R. A. Surmenev and I. V. Antoniac, Bioceramic Coatings for Metallic Implants, *Handbook of Bioceramics and Biocomposites*, 2016, 703–733.
- 2 R. A. Surmenev, M. A. Surmeneva and A. A. Ivanova, Significance of Calcium Phosphate Coatings for the Enhancement of New Bone Osteogenesis – a Review, *Acta Biomater.*, 2014, **10**, 557–579.
- 3 Y. Li, S. Zou, D. Wang, G. Khan, C. Bao and J. Hu, The Effect of Hydrofluoric Acid Treatment on Titanium Implant Osseointegration in Ovariectomized Rats, *Biomaterials*, 2010, **31**, 3266–3273.
- 4 M. R. Khan, N. Donos, V. Salih and P. M. Brett, The Enhanced Modulation of Key Bone Matrix Components by Modified Titanium Implant Surfaces, *Bone*, 2012, **50**, 1–8.
- 5 B. León and J. A. Jansen, *Thin Calcium Phosphate Coatings for Medical Implants*, Springer, New York, 2009.
- 6 X. Wei, C. Fu, K. Savino and M. Z. Yates, Fully Dense Yttrium-Substituted Hydroxyapatite Coatings with Aligned Crystal Domains, *Cryst. Growth Des.*, 2012, **12**, 217–223.
- 7 F. J. Garciasanz, M. B. Mayor, J. L. Aris, J. Pou and B. León, Pérez-Amor, M. Hydroxyapatite Coatings a Comparative Study between Plasma-Spray and Pulsed Laser Deposition Techniques, *J. Mater. Sci.: Mater. Med.*, 1997, **8**, 861–865.
- 8 B. Cofino, P. Fogarassy, P. Millet and A. Lodini, Thermal Residual Stresses Near the Interface Between Plasma-Sprayed Hydroxyapatite Coating and Titanium Substrate: Finite Element Analysis and Synchrotron Radiation Measurements, *J. Biomed. Mater. Res.*, 2004, **70**, 20–27.
- 9 J. Terra, E. R. Dourado, J. G. Eon, D. E. Ellis, G. Gonzalez and A. M. Rossi, The Structure of Strontium-Doped Hydroxyapatite: An Experimental and Theoretical Study, *Phys. Chem. Chem. Phys.*, 2009, **11**, 568–577.
- 10 I. Y. Grubova, M. A. Surmeneva, A. A. Ivanova, K. Kravchuk, O. Prymak, M. Epple, V. Buck and R. A. Surmenev, The Effect of Patterned Titanium Substrates on the Properties of Silver-Doped Hydroxyapatite Coatings, *Surf. Coat. Technol.*, 2015, **276**, 595–601.
- 11 I. Grubova, T. Priamushko, E. Chudinova, M. Surmeneva, O. Korneva, M. Epple, O. Prymak, I. Shulepov and R. Surmenev, Formation and Characterization of Crystalline Hydroxyapatite Coating with the (002) Texture, *IOP Conf. Ser.: Mater. Sci. Eng.*, 2016, **116**, 012016.
- 12 A. A. Ivanova, M. A. Surmeneva, I. Y. Grubova, A. A. Sharonova, V. F. Pichugin, M. V. Chaikina, V. Buck, O. Prymak and M. Epple, Surmenev, R. A. Influence of the Substrate Bias on the Stoichiometry and Structure of RF-Magnetron Sputter-Deposited Silver-Containing Calcium Phosphate Coatings, *Materialwiss. Werkstofftech.*, 2013, **44**, 218–225.
- 13 R. A. A. Surmenev, Review of Plasma-Assisted Methods for Calcium Phosphate-Based Coatings Fabrication, *Surf. Coat. Technol.*, 2012, **206**, 2035–2056.
- 14 S. Grimme, Accurate Description of van der Waals Complexes by Density Functional Theory Including Empirical Corrections, *J. Comput. Chem.*, 2004, **25**, 1463–1473.
- 15 S. Grimme, Semiempirical GGA-Type Density Functional Constructed with a Long-Range Dispersion Correction, *J. Comput. Chem.*, 2006, **27**, 1787–1799.
- 16 F. Ortmann, F. Bechstedt and W. G. Schmidt, Semiempirical van der Waals Correction to the Density Functional Description of Solids and Molecular Structures, *Phys. Rev. B: Condens. Matter Mater. Phys.*, 2006, **73**, 205101.
- 17 Q. Wu, Q. Wu and W. Yang, Empirical Correction to Density Functional Theory for van der Waals Interactions, *J. Chem. Phys.*, 2002, **116**, 515–524.

- 18 A. D. Becke and E. R. Johnson, Exchange-Hole Dipole Moment and the Dispersion Interaction, *J. Chem. Phys.*, 2005, **122**, 154104.
- 19 A. D. Becke and E. R. Johnson, A Density-Functional Model of the Dispersion Interaction, *J. Chem. Phys.*, 2005, **123**, 154101.
- 20 E. R. Johnson and A. D. Becke, A Post-Hartree–Fock Model of Intermolecular Interactions, *J. Chem. Phys.*, 2005, **123**, 024101.
- 21 T. Sato and H. Nakai, Density Functional Method Including Weak Interactions: Dispersion Coefficients Based on the Local Response Approximation, *J. Chem. Phys.*, 2009, **131**, 224104.
- 22 P. L. Silvestrelli, Van der Waals Interactions in DFT Made Easy by Wannier Functions, *Phys. Rev. Lett.*, 2008, **100**, 053002.
- 23 A. Tkatchenko and M. Scheffler, Accurate Molecular van der Waals Interactions from Ground-State Electron Density and Free-Atom Reference Data, *Phys. Rev. Lett.*, 2009, **102**, 073005.
- 24 M. Dion, H. Rydberg, E. Schrödinger, D. C. Langreth and B. I. Lundqvist, Van der Waals Density Functional for General Geometries, *Phys. Rev. Lett.*, 2004, **92**, 246401.
- 25 K. Lee, E. D. Murray, L. Kong, B. I. Lundqvist and D. C. Langreth, Higher-Accuracy van der Waals Density Functional, *Phys. Rev. B: Condens. Matter Mater. Phys.*, 2010, **82**, 081101.
- 26 S. Grimme, J. Antony, S. Ehrlich and H. Krieg, A Consistent and Accurate Ab Initio Parametrization of Density Functional Dispersion Correction (DFT-D) for the 94 Elements H–Pu, *J. Chem. Phys.*, 2010, **132**, 154104.
- 27 L. A. Goerigk, *Comprehensive Overview of the DFT-D3 London-Dispersion Correction. Non-Covalent Interactions in Quantum Chemistry and Physics*, Elsevier, 2017, pp. 195–219.
- 28 I. Y. Grubova, M. A. Surmeneva, S. Huygh, R. A. Surmenev and E. C. Neyts, Effects of Silicon Doping on Strengthening Adhesion at the Interface of the Hydroxyapatite–Titanium Biocomposite: A First-Principles Study, *Comput. Mater. Sci.*, 2019, **159**, 228–234.
- 29 G. Kresse and J. Hafner, Ab Initio Molecular Dynamics for Liquid Metals, *Phys. Rev. B: Condens. Matter Mater. Phys.*, 1993, **47**, 558–561.
- 30 G. Kresse and J. Furthmüller, Efficiency of Ab-Initio Total Energy Calculations for Metals and Semiconductors Using a Plane-Wave Basis Set, *Comput. Mater. Sci.*, 1996, **6**, 15–50.
- 31 G. Kresse and J. Furthmüller, Efficient Iterative Schemes for Ab Initio Total-Energy Calculations Using a Plane-Wave Basis Set, *Phys. Rev. B: Condens. Matter Mater. Phys.*, 1996, **54**, 11169–11186.
- 32 G. Kresse and J. Hafner, Norm-Conserving and Ultrasoft Pseudopotentials for First-Row and Transition Elements, *J. Phys.: Condens. Matter*, 1994, **6**, 8245–8257.
- 33 G. Kresse and D. Joubert, From Ultrasoft Pseudopotentials to the Projector Augmented-Wave Method, *Phys. Rev. B: Condens. Matter Mater. Phys.*, 1999, **59**, 1758–1775.
- 34 J. P. Perdew, K. Burke and M. Ernzerhof, Generalized Gradient Approximation Made Simple, *Phys. Rev. Lett.*, 1996, **77**, 3865–3868.
- 35 J. P. Perdew, K. Burke and M. Ernzerhof, Generalized Gradient Approximation Made Simple, *Phys. Rev. Lett.*, 1997, **78**, 1396.
- 36 P. E. Blöchl, O. Jepsen and O. K. Andersen, Improved Tetrahedron Method for Brillouin-Zone Integrations, *Phys. Rev. B: Condens. Matter Mater. Phys.*, 1994, **49**, 16223–16233.
- 37 I. Y. Grubova, M. A. Surmeneva, S. Huygh, R. A. Surmenev and E. C. Neyts, Density Functional Theory Study of Interface Interactions in Hydroxyapatite/Rutile Composites for Biomedical Applications, *J. Phys. Chem. C*, 2017, **121**, 15687–15695.
- 38 K. Momma and F. Izumi, VESTA 3 for Three-Dimensional Visualization of Crystal, Volumetric and Morphology Data, *J. Appl. Crystallogr.*, 2011, **44**, 1272–1276.
- 39 M. W. Finnis, The Theory of Metal–Ceramic Interfaces, *J. Phys.: Condens. Matter*, 1996, **8**, 5811–5836.
- 40 M. A. Trubitsyn, N. G. Gabruk, L. van Thuan and D. van Dat, The Comparative Characteristic of Physical, Chemical and Bioactive Properties of the Synthesized Hydroxyapatites, *Global J. Pharmacol.*, 2013, **7**, 342–347.
- 41 J. P. Sun, J. Dai, Y. Song, Y. Wang and R. Yang, Affinity of the Interface between Hydroxyapatite (0001) and Titanium (0001) Surfaces: A First-Principles Investigation, *ACS Appl. Mater. Interfaces*, 2014, **6**, 20738–20751.